Optics Letters

Few-mode erbium-doped fiber amplifier with photonic lantern for pump spatial mode control

G. Lopez-Galmiche,[1,2,*] Z. Sanjabi Eznaveh,[1] J. E. Antonio-Lopez,[1] A. M. Velazquez Benitez,[1] J. Rodriguez Asomoza,[1,3] J. J. Sanchez Mondragon,[2] C. Gonnet,[4] P. Sillard,[4] G. Li,[1] A. Schülzgen,[1] C. M. Okonkwo,[5] and R. Amezcua Correa[1]

[1]CREOL, The College of Optics and Photonics, the University of Central Florida, Orlando, Florida 32816, USA
[2]Instituto Nacional de Astrofísica Óptica y Electrónica (INAOE), A.P. 51 y 216, Tonantzintla, Puebla 7200, Mexico
[3]Universidad de las Americas Puebla, Sta. Catarina, Tonantzintla, Puebla 7200, Mexico
[4]Prysmian Group, Parc des Industries Artois Flandres, 644 Boulevard Est, Billy Berclau, 62092 Haisnes Cedex, France
[5]COBRA Research Institute, Eindhoven University of Technology, The Netherlands
*Corresponding author: gisela.lopezgalmiche@ucf.edu

Received 15 February 2016; revised 26 April 2016; accepted 26 April 2016; posted 2 May 2016 (Doc. ID 259498); published 26 May 2016

We demonstrate a few-mode erbium-doped fiber amplifier employing a mode-selective photonic lantern for controlling the modal content of the pump light. Amplification of six spatial modes in a 5 m long erbium-doped fiber to ~6.2 dBm average power is obtained while maintaining high modal fidelity. Through mode-selective forward pumping of the two degenerate LP_{21} modes operating at 976 nm, differential modal gains of <1 dB between all modes and signal gains of ~16 dB at 1550 nm are achieved. In addition, low differential modal gain for near-full C-band operation is demonstrated.

OCIS codes: (060.0060) Fiber optics and optical communications; (060.2410) Fibers, erbium; (060.2320) Fiber optics amplifiers and oscillators; (060.4230) Multiplexing.

http://dx.doi.org/10.1364/OL.41.002588

Research on space division multiplexing (SDM) in few-mode fibers (FMFs), multimode fibers, and multicore fibers has been on the increase in recent years [1–7]. SDM transmission promises to enable a significant increase in data transport within a single optical fiber by exploiting multiple spatial paths as independent data channels [1–7]. Within the context of multimode fiber transmissions, the key factors to record experiments demonstrating 3, 6, 10, and 15 spatial mode transmissions [1–3] are the development of new FMFs [7–11] and new components such as compact mode multiplexers [1,12]. Fiber-based photonic lanterns (PLs) and mode-selective photonic lanterns (MSPLs) have emerged as promising all-fiber spatial multiplexers due to their ability to be directly spliced onto the transmitting fibers [12–18]. To this end, extensive research has focused on improving fabrication techniques so as to achieve low-loss coupling into the transmission fiber with minimal mode-dependent loss. To fabricate a MSPL, a number of fibers with dissimilar fundamental mode propagation constants are encapsulated by a low-refractive-index capillary, whose number of supported modes can be scaled with the number of input fibers employed [12,14,15]. This arrangement of N fibers is adiabatically tapered down to a multimode fiber structure. In this case, the fundamental modes of the single-mode waveguides are mapped onto the modes of the multimode waveguide.

In addition to the key passive components under development, fiber amplifiers supporting a large number of spatial channels are crucial for the large capacity possible with SDM systems to be extended over longer transmission distances [1,19–21]. For few-mode erbium-doped fiber amplifiers (FM-EDFAs), the main challenge is achieving adequate gain with low differential modal gain (DMG) between all the supported spatial channels over the full C-band. In this regard, the ability to equalize the gain between all modes is critical to the overall performance of the SDM transmission system as a high differential modal gain translates to high mode-dependent loss, which can result in system outage.

Two main design strategies have been proposed for improving the mode-dependent gain performance of FM-EDFAs. First, by controlling the pump modal content, and second, by controlling the erbium-doped fiber (EDF) doping profile [22–24]. Thus far, FM-EDFAs with low differential modal gain have been demonstrated by mode-selective pumping of the EDF employing phase plates to generate the required higher order pump modes or by using cladding pumping schemes to homogenize the pump intensity in the core region [25,26]. Recently, a ring-doped EDFA supporting six spatial modes was demonstrated [27]. In this case, by using a tailored erbium-doping profile in combination with a mode-selective pumping configuration, low DMG of <2 dB and reconfigurable gain control were demonstrated. However, a phase-plate-based pump control requires fairly bulky systems and has serious drawbacks in terms of coupling losses, which limits scalability.

In this work, we demonstrate an all-fiber six-mode amplifier with low DMG by using a MSPL for controlling the modal

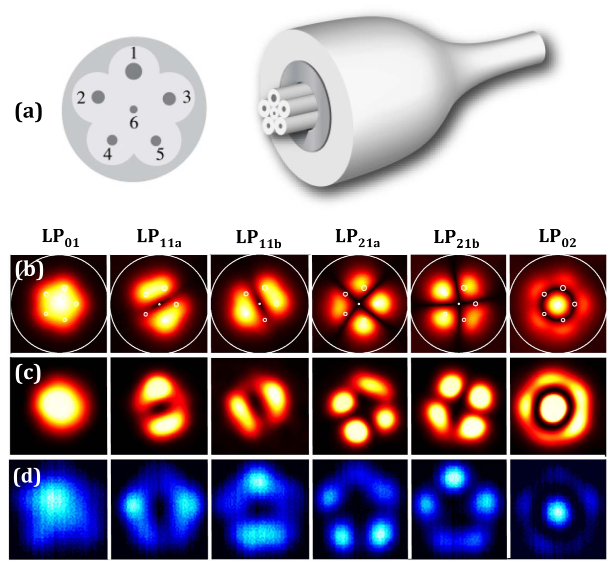

Fig. 1. (a) Schematic of the six-mode MSPL. Near-field mode profiles at the PL output (b) calculated using BPM at 1550 nm, (c) measured at 1550 nm, and (d) measured at 976 nm.

content of the pump in a copropagating pumping scheme. In this regard, the MSPL multiplexer is critical to the proposed all-fiber FM-EDFA. The schematic of the employed MSPL is shown in Fig. 1(a). The device supports six LP modes (LP_{01}, LP_{11a}, LP_{11b}, LP_{21a}, LP_{21b}, and LP_{02}). The geometrical configuration and the fabrication process were optimized to minimize insertion and mode-dependent losses as outlined in [17].

Table 1 summarizes the individual core diameters and their positions in the MSPL, as depicted in Fig. 1(a). The core diameter at the lantern waist is ∼17 μm. The refractive index contrast of the graded-index cores and the fluorine-doped silica capillary are 16×10^{-3} and -9×10^{-3}, respectively. An adiabatic transition ensures that light in the Nth fiber evolves to the Nth mode at the facet of the MSPL with minimal loss. It is highlighted that the length required to achieve an adiabatic transition can be considerably reduced by using graded-index and/or reduced-outer diameter fibers [16–18]. The six-mode MSPL was first simulated using a beam propagation method (BPM). The simulated and measured near-field mode profiles at the MSPL output for a wavelength of 1550 nm are presented in Figs. 1(b) and 1(c), respectively. Additionally, the measured output near-field mode profiles at the pump wavelength are displayed in Fig. 1(d).

A step index EDF fabricated in-house was used to investigate the MSPL few-mode amplifier. The refractive index profile of the employed EDF, measured using a refractive index profiler, is presented in Fig. 2(a). The EDF has an outer diameter of 163 μm and a core diameter of 13 μm. The estimated NA of

Table 1. Photonic Lantern Input Fiber Parameters

Fiber Position	1	2	3	4	5	6
Mode	LP_{01}	LP_{11a}	LP_{1b}	LP_{21a}	LP_{2b}	LP_{02}
Core dia. (μm)	22	18	18	15	15	6

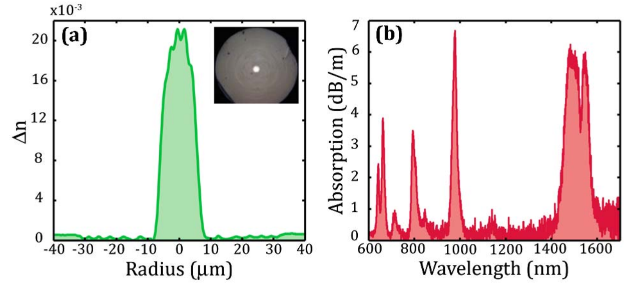

Fig. 2. (a) Measured refractive index of the EDF with core and cladding diameters of 13 μm and 163 μm, respectively. (b) Measured absorption spectrum using the cutback method.

the erbium-doped core is ∼0.24, ensuring that more than six modes are supported at the signal wavelength. Figure 2(b) shows the absorption spectrum of the EDF obtained through a cutback measurement using a fiber-based supercontinuum source and an optical spectrum analyzer (OSA). The absorption coefficient at 976 nm was measured to be ∼6.7 dB/m.

To experimentally verify the performance of the MSPL-based FM-EDFA, the setup depicted in Fig. 3 was employed. A tunable semiconductor laser generates the signal. After polarization controllers and an optical isolator, the fundamental mode is coupled to one input branch of the MSPL multiplexer, which converts the signal into one of the six supported modes. Two fiber-coupled 976 nm single-mode laser diodes were employed to pump the EDFA by simultaneously injecting the LP_{21a} and LP_{21b} modes. Equal pump powers were launched to each mode in a codirectional pumping configuration. WDM couplers (976 nm/1550 nm) are used to couple both pump and signal to the MSPL input corresponding to the degenerate LP21 modes. The tapered facet of the MSPL multiplexer was then spliced to an intermediate 1 m long passive FMF with a 15 μm core diameter and a 125 μm outer diameter. Finally, the passive FMF was spliced directly to a 5 m long FM-EDF.

The output of the amplifier was characterized using a charge-coupled device camera, an OSA, and a power meter. The modal gain of the EDFA as a function of total pump power ($LP_{21a} + LP_{21b}$) for a 0.1 mW input signal at 1550 nm was measured. Figure 4(a) shows the gain evolution for each spatial mode individually amplified. For low pump powers <200 mW, we measured DMG values of >4 dB between the six supported modes. The relatively large DMG observed at low pump powers is dominated by the mode-dependent losses of the MSPL and the mode-dependent losses at the splice points to the FMF and to the EDF. Interestingly, as the pump

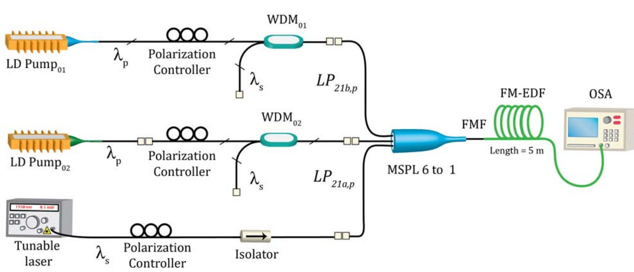

Fig. 3. Schematic diagram of the six-mode EDFA pumped by the LP_{21a} and LP_{21b} modes.

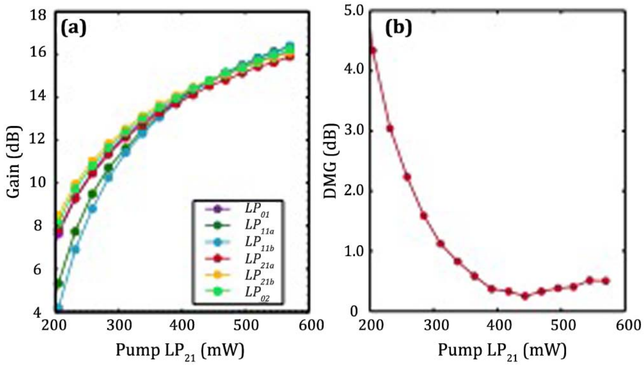

Fig. 4. Amplification of each mode, launched individually, for a signal wavelength of 1550 nm. (a) Measured individual modal gain, and (b) DMG as a function of total pump power ($LP_{21a} + LP_{21b}$).

power increases, a clear reduction in the DMG is observed. We note that similar effects have been observed by Jung, *et al.* [27]. Under high pump power conditions, the amplifier moves toward full inversion. As a result, all spatial channels achieve larger gain. Moreover, for increasing pump powers, higher order modes experience a larger gain increase relative to the fundamental mode due to the employed pump beam profile, thereby lowering the DMG. Figure 4(b) indicates that the minimum measured DMG value was 0.25 dB when a pump power of ~458 mW is launched into the EDFA. For the maximum available pump power (~570 mW), a DMG of 0.5 dB was achieved. In addition, an average amplification gain of ~16 dB between all six spatial modes was achieved for ~570 mW of pump power.

The signal modes prior to and after amplification and the pump modes were studied by capturing their transverse mode profiles using an infrared camera. Figures 5(a) and 5(b) show the measured near-field signal mode profiles before and after amplification at the output of the 5 m FM-EDF. These images clearly confirm that the spatial profiles of the amplified signal modes are well preserved at the EDFA output. The phase changes seen from the mode profiles of the degenerate modes (LP_{11} and LP_{21}) prior to and after amplification are due to the amplification process itself. It is to be noted that the spatial distribution of the amplified modes indicates minimal distortion and mode mixing that could be attributed to the amplifier. The pump spatial profiles for the LP_{21a} and LP_{21b}

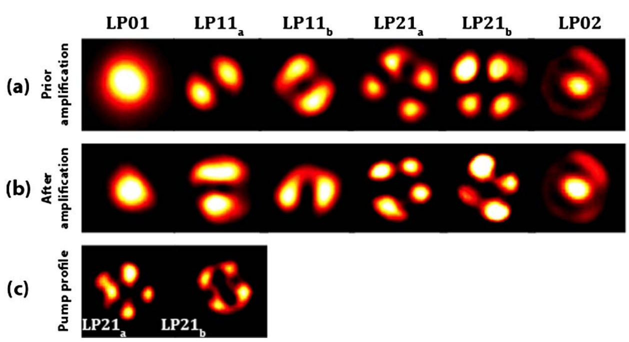

Fig. 5. Near-field signal-mode profiles at the EDF output for a wavelength of 1550 nm (a) prior to amplification and (b) after amplification. (c) Pump near-field mode profiles LP_{21ab} at 976 nm captured at the EDF output.

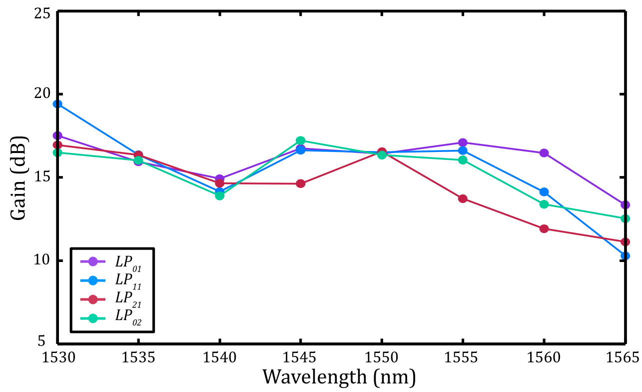

Fig. 6. Modal gain as a function of wavelength across the C-band. For input signal power of 0.1 mW and pump power of 570 mW.

modes at the output of the EDFA are presented in Fig. 5(c), showing clean spatial distributions and confirming high-efficiency coupling of the pump light to the selected modes.

In order to evaluate the DMG of the FM-EDFA at different wavelengths, the input signal was scanned across the C-band (1535 to 1565 nm) in 5 nm steps. The pump and signal powers were adjusted to 570 mW and 0.1 mW, respectively. Figure 6 shows the measured modal gain across the C-band for all modes injected individually. An average DMG of approximately 2.3 dB is achieved.

It is noted that gains of 10.3 and 19.4 dB were obtained at the edges of the C-band. For a wavelength range of 1535 to 1550 nm, DMG values between 2.58 and 0.23 dB were measured. Further optimization of the pump modal content and/or the EDF length could potentially allow the gain to be increased while maintaining a low DMG.

In summary, we have demonstrated an integrated photonic lantern FM-EDFA supporting six spatial modes with low DMG. Spatial mode control of the pump is achieved using an all-fiber device. The presented mode-selective pumping scheme yields remarkably low DMG values and adequate gain levels. In addition, the signal mode profiles were conserved during the amplification process with relatively low spatial degradation. The proposed MSPL-EDFA is a compact system with the potential of providing reconfigurable mode-dependent gain. In addition, this amplifier configuration could be scaled to support a larger number of spatial modes without compromising the mode-dependent gain crucial for long-distance FMF transmission.

Funding. Army Research Office (ARO) (W911NF-13-1-0283, W911NF-12-1-0450); High Energy Laser Join Technology Office (HEL-JTO) (W911NF-12-1-0450); Air Force Office of Scientific Research (AFOSR) (FA9550-15-10041); Consejo Nacional de Ciencia y Tecnología (CONACYT).

REFERENCES

1. D. J. Richardson, J. M. Fini, and L. E. Nelson, Nat. Photonics **7**, 354 (2013).
2. P. J. Winzer, IEEE Photon. Technol. Lett. **23**, 851 (2011).
3. S. Randel, R. Ryf, A. Sierra, P. J. Winzer, A. H. Gnauck, C. A. Bolle, R.-J. Essiambre, D. W. Peckham, A. McCurdy, and R. Lingle, Opt. Express **19**, 16697 (2011).

4. R. G. H. van Uden, R. A. Correa, E. A. Lopez, F. M. Huijskens, C. Xia, G. Li, A. Schulzgen, H. de Waardt, A. M. J. Koonen, and C. M. Okonkwo, Nat. Photonics **8**, 865 (2014).
5. R. Ryf, S. Randel, A. H. Gnauck, C. Bolle, A. Sierra, S. Mumtaz, M. Esmaeelpour, E. C. Burrows, R.-J. Essiambre, P. J. Winzer, D. W. Peckham, A. H. McCurdy, and R. Lingle, J. Lightwave Technol. **30**, 521 (2012).
6. B. Zhu, J. M. Fini, M. F. Yan, X. Liu, S. Chandrasekhar, T. F. Taunay, M. Fishteyn, E. M. Monberg, and F. V. Dimarcello, J. Lightwave Technol. **30**, 486492 (2012).
7. P. Sillard, M. Bigot-Astruc, and D. Molin, J. Lightwave Technol. **32**, 2824 (2014).
8. R. Ryf, S. Randel, N. K. Fontaine, M. Montoliu, E. Burrows, S. Chandrasekhar, A. H. Gnauck, C. Xie, R. Essiambre, P. Winzer, R. Delbue, P. Pupalaikis, A. Sureka, Y. Sun, L. Gruner-Nielsen, R. V. Jensen, and R. Lingle, "32-bit/s/Hz spectral efficiency WDM transmission over 177-km few-mode fiber," in *Optical Fiber Communication Conference*, Anaheim, California, 2013, paper PDP5A.1.
9. J. van Weerdenburg, A. Velàzquez-Benitez, R. van Uden, P. Sillard, D. Molin, A. Amezcua-Correa, E. Antonio-Lopez, M. Kuschnerov, F. Huijskens, H. de Waardt, T. Koonen, R. Amezcua-Correa, and C. Okonkwo, Opt. Express **23**, 24759 (2015).
10. N. K. Fontaine, R. Ryf, H. Chen, A. V. Benitez, B. Guan, R. Scott, B. Ercan, S. J. B. Yoo, L. E. Grüner-Nielsen, Y. Sun, R. Lingle, E. Antonio-Lopez, and R. Amezcua-Correa, "30 × 30 MIMO transmission over 15 spatial modes," in *Optical Fiber Communication Conference*, Los Angeles, California, 2015, paper Th5C.1.
11. P. Sillard, D. Molin, M. Bigot-Astruc, K. De Jongh, F. Achten, A. M. Velazquez-Benitez, R. Amezcua-Correa, and C. M. Okonkwo, J. Lightwave Technol. **34**, 425 (2016).
12. S. G. Leon-Saval, N. K. Fontaine, J. R. Salazar-Gil, B. Ercan, R. Ryf, and J. Bland-Hawthorn, Opt. Express **22**, 1036 (2014).
13. S. G. Leon-Saval, Opt. Express **18**, 8430 (2010).
14. S. G. Leon-Saval, Nanophotonics **2**, 429 (2013).
15. T. A. Birks, I. Gris-Sánchez, S. Yerolatsitis, S. G. Leon-Saval, and R. R. Thomson, Adv. Opt. Photon. **7**, 107 (2015).
16. S. Yerolatsitis, I. Gris-Sánchez, and T. A. Birks, Opt. Express **22**, 608 (2014).
17. A. M. Velazquez-Benitez, J. C. Alvarado, G. Lopez-Galmiche, J. E. Antonio-Lopez, J. Hernandez-Cordero, J. Sanchez-Mondragon, P. Sillard, C. M. Okonkwo, and R. Amezcua-Correa, Opt. Lett. **40**, 1663 (2015).
18. B. Huang, N. K. Fontaine, R. Ryf, B. B. Guan, S. G. Leon-Saval, R. Shubochkin, Y. Sun, R. Lingle, and G. F. Li, Opt. Express **23**, 224 (2015).
19. V. A. J. M. Sleiffer, Y. Jung, V. Veljanovski, R. G. H. van Uden, M. Kuschnerov, H. Chen, B. Inan, L. Grüner Nielsen, Y. Sun, D. J. Richardson, S. U. Alam, F. Poletti, J. K. Sahu, A. Dhar, A. M. J. Koonen, B. Corbett, R. Winfield, A. D. Ellis, and H. de Waardt, Opt. Express **20**, B428 (2012).
20. N. Bai, E. Ip, Y.-K. Huang, E. Mateo, F. Yaman, M.-J. Li, S. Bickham, S. Ten, J. Liñares, C. Montero, V. Moreno, X. Prieto, V. Tse, K. Chung, A. Lau, H.-Y. Tam, C. Lu, Y. Luo, G.-D. Peng, G. Li, and T. Wang, Opt. Express **20**, 2668 (2012).
21. Y. Jung, S. Alam, Z. Li, A. Dhar, D. Giles, I. P. Giles, J. K. Sahu, F. Poletti, L. Grüner-Nielsen, and D. J. Richardson, Opt. Express **19**, B952 (2011).
22. N. Bai, E. Ip, T. Wang, and G. Li, Opt. Express **19**, 16601 (2011).
23. Q. Kang, E. L. Lim, Y. Jung, J. K. Sahu, F. Poletti, C. Baskiotis, S. U. Alam, and D. J. Richardson, Opt. Express **20**, 20835 (2012).
24. L. Bigot, G. Le Cocq, and Y. Quiquempois, J. Lightwave Technol. **33**, 588 (2015).
25. Y. Jung, E. L. Lim, Q. Kang, T. C. May-Smith, N. H. L. Wong, R. Standish, F. Poletti, J. K. Sahu, S. U. Alam, and D. J. Richardson, Opt. Express **22**, 29008 (2014).
26. N. K. Fontaine, B. Huang, Z. Sanjabi Eznaveh, H. Chen, C. Jin, B. Ercan, A. Velázquez-Benetez, S. H. Chang, R. Ryf, A. Schülzgen, J. Carlos Alvarado, P. Sillard, C. Gonnet, E. Antonio-Lopez, and R. Amezcua Correa, in *Optical Fiber Communication Conference*, OSA Technical Digest (Optical Society of America, 2016), paper Th5A.4.
27. Y. Jung, Q. Kang, J. K. Sahu, B. Corbett, J. O'Callagham, F. Poletti, S. U. Alam, and D. J. Richardson, Photon. Technol. Lett. **26**, 1100 (2014).